

# Study of the $P$ -wave charmonium state $\chi_{cJ}$ in $\psi(2S)$ decays

J. Z. Bai<sup>1</sup>, J. G. Bian<sup>1</sup>, I. Blum<sup>11</sup>, Z. W. Chai<sup>1</sup>, G. P. Chen<sup>1</sup>, H. F. Chen<sup>10</sup>, J. Chen<sup>3</sup>, J. C. Chen<sup>1</sup>, Y. Chen<sup>1</sup>, Y. B. Chen<sup>1</sup>, Y. Q. Chen<sup>1</sup>, B. S. Cheng<sup>1</sup>, X. Z. Cui<sup>1</sup>, H. L. Ding<sup>1</sup>, L. Y. Ding<sup>1</sup>, L. Y. Dong<sup>1</sup>, Z. Z. Du<sup>1</sup>, W. Dunwoodie<sup>7</sup>, S. Feng<sup>1</sup>, C. S. Gao<sup>1</sup>, M. L. Gao<sup>1</sup>, S. Q. Gao<sup>1</sup>, P. Gratton<sup>11</sup>, J. H. Gu<sup>1</sup>, S. D. Gu<sup>1</sup>, W. X. Gu<sup>1</sup>, Y. F. Gu<sup>1</sup>, Y. N. Guo<sup>1</sup>, S. W. Han<sup>1</sup>, Y. Han<sup>1</sup>, F. A. Harris<sup>8</sup>, J. He<sup>1</sup>, J. T. He<sup>1</sup>, M. He<sup>5</sup>, D. G. Hitlin<sup>2</sup>, G. Y. Hu<sup>1</sup>, H. M. Hu<sup>1</sup>, J. L. Hu<sup>12,1</sup>, Q. H. Hu<sup>1</sup>, T. Hu<sup>1</sup>, X. Q. Hu<sup>1</sup>, J. D. Huang<sup>1</sup>, Y. Z. Huang<sup>1</sup>, J. M. Izen<sup>11</sup>, C. H. Jiang<sup>1</sup>, Y. Jin<sup>1</sup>, Z. J. Ke<sup>1</sup>, M. H. Kelsey<sup>2</sup>, B. K. Kim<sup>11</sup>, D. Kong<sup>8</sup>, Y. F. Lai<sup>1</sup>, P. F. Lang<sup>1</sup>, A. Lankford<sup>9</sup>, C. G. Li<sup>1</sup>, D. Li<sup>1</sup>, H. B. Li<sup>1</sup>, J. Li<sup>1</sup>, P. Q. Li<sup>1</sup>, R. B. Li<sup>1</sup>, W. Li<sup>1</sup>, W. D. Li<sup>1</sup>, W. G. Li<sup>1</sup>, X. H. Li<sup>1</sup>, X. N. Li<sup>1</sup>, H. M. Liu<sup>1</sup>, J. Liu<sup>1</sup>, J. H. Liu<sup>1</sup>, R. G. Liu<sup>1</sup>, Y. Liu<sup>1</sup>, X. C. Lou<sup>11</sup>, B. Lowery<sup>11</sup>, F. Lu<sup>1</sup>, J. G. Lu<sup>1</sup>, J. Y. Lu<sup>1</sup>, L. C. Lu<sup>1</sup>, C. H. Luo<sup>1</sup>, A. M. Ma<sup>1</sup>, E. C. Ma<sup>1</sup>, J. M. Ma<sup>1</sup>, R. Malchow<sup>3</sup>, H. S. Mao<sup>1</sup>, Z. P. Mao<sup>1</sup>, X. C. Meng<sup>1</sup>, J. Nie<sup>1</sup>, S. L. Olsen<sup>8</sup>, J. Oyang<sup>2</sup>, D. Paluselli<sup>8</sup>, L. J. Pan<sup>8</sup>, J. Panetta<sup>2</sup>, F. Porter<sup>2</sup>, N. D. Qi<sup>1</sup>, X. R. Qi<sup>1</sup>, C. D. Qian<sup>6</sup>, J. F. Qiu<sup>1</sup>, Y. H. Qu<sup>1</sup>, Y. K. Que<sup>1</sup>, G. Rong<sup>1</sup>, M. Schernau<sup>9</sup>, Y. Y. Shao<sup>1</sup>, B. W. Shen<sup>1</sup>, D. L. Shen<sup>1</sup>, H. Shen<sup>1</sup>, X. Y. Shen<sup>1</sup>, H. Y. Sheng<sup>1</sup>, H. Z. Shi<sup>1</sup>, X. F. Song<sup>1</sup>, J. Standifird<sup>11</sup>, F. Sun<sup>1</sup>, H. S. Sun<sup>1</sup>, S. Q. Tang<sup>1</sup>, W. Toki<sup>3</sup>, G. L. Tong<sup>1</sup>, G. Varner<sup>8</sup>, F. Wang<sup>1</sup>, L. S. Wang<sup>1</sup>, L. Z. Wang<sup>1</sup>, M. Wang<sup>1</sup>, Meng Wang<sup>1</sup>, P. Wang<sup>1</sup>, P. L. Wang<sup>1</sup>, S. M. Wang<sup>1</sup>, T. J. Wang<sup>1†</sup>, Y. Y. Wang<sup>1</sup>, M. Weaver<sup>2</sup>, C. L. Wei<sup>1</sup>, Y. G. Wu<sup>1</sup>, D. M. Xi<sup>1</sup>, X. M. Xia<sup>1</sup>, P. P. Xie<sup>1</sup>, Y. Xie<sup>1</sup>, Y. H. Xie<sup>1</sup>, W. J. Xiong<sup>1</sup>, C. C. Xu<sup>1</sup>, G. F. Xu<sup>1</sup>, S. T. Xue<sup>1</sup>, J. Yan<sup>1</sup>, W. G. Yan<sup>1</sup>, C. M. Yang<sup>1</sup>, C. Y. Yang<sup>1</sup>, J. Yang<sup>1</sup>, W. Yang<sup>3</sup>, X. F. Yang<sup>1</sup>, M. H. Ye<sup>1</sup>, S. W. Ye<sup>10</sup>, Y. X. Ye<sup>10</sup>, K. Yi<sup>1</sup>, C. S. Yu<sup>1</sup>, C. X. Yu<sup>1</sup>, Y. H. Yu<sup>4</sup>, Z. Q. Yu<sup>1</sup>, Z. T. Yu<sup>1</sup>, C. Z. Yuan<sup>12,1</sup>, Y. Yuan<sup>1</sup>, B. Y. Zhang<sup>1</sup>, C. C. Zhang<sup>1</sup>, D. H. Zhang<sup>1</sup>, Dehong Zhang<sup>1</sup>, H. L. Zhang<sup>1</sup>, J. Zhang<sup>1</sup>, J. L. Zhang<sup>1</sup>, J. W. Zhang<sup>1</sup>, L. S. Zhang<sup>1</sup>, Q. J. Zhang<sup>1</sup>, S. Q. Zhang<sup>1</sup>, X. Y. Zhang<sup>5</sup>, Y. Zhang<sup>1</sup>, Y. Y. Zhang<sup>1</sup>, D. X. Zhao<sup>1</sup>, H. W. Zhao<sup>1</sup>, J. W. Zhao<sup>1</sup>, M. Zhao<sup>1</sup>, W. R. Zhao<sup>1</sup>, Z. G. Zhao<sup>1</sup>, J. P. Zheng<sup>1</sup>, L. S. Zheng<sup>1</sup>, Z. P. Zheng<sup>1</sup>, G. P. Zhou<sup>1</sup>, H. S. Zhou<sup>1</sup>, L. Zhou<sup>1</sup>, Q. M. Zhu<sup>1</sup>, Y. C. Zhu<sup>1</sup>, Y. S. Zhu<sup>1</sup>, B. A. Zhuang<sup>1</sup>

(BES Collaboration)

<sup>1</sup>*Institute of High Energy Physics, Beijing 100039, People's Republic of China*

<sup>2</sup>*California Institute of Technology, Pasadena, California 91125*

<sup>3</sup>*Colorado State University, Fort Collins, Colorado 80523*

<sup>4</sup>*Hangzhou University, Hangzhou 310028, People's Republic of China*

<sup>5</sup>*Shandong University, Jinan 250100, People's Republic of China*

<sup>6</sup>*Shanghai Jiaotong University, Shanghai 200030, People's Republic of China*

<sup>7</sup>*Stanford Linear Accelerator Center, Stanford, California 94309*

<sup>8</sup>*University of Hawaii, Honolulu, Hawaii 96822*

<sup>9</sup>*University of California at Irvine, Irvine, California 92717*

<sup>10</sup>*University of Science and Technology of China, Hefei 230026, People's Republic of China*

<sup>11</sup>*University of Texas at Dallas, Richardson, Texas 75083-0688*

<sup>12</sup>*China Center of Advanced Science and Technology (World Laboratory), Beijing 100080, People's Republic of China*

(Received 1 July 1998)

## Abstract

The processes  $\psi(2S) \rightarrow \gamma\pi^+\pi^-$ ,  $\gamma K^+K^-$  and  $\gamma p\bar{p}$  have been studied using a sample of  $3.79 \times 10^6$   $\psi(2S)$  decays. We determine the total width of the  $\chi_{c0}$  to be  $\Gamma_{\chi_{c0}}^{tot} = 14.3 \pm 2.0 \pm 3.0$  MeV. We present the first measurement of the branching fraction  $B(\chi_{c0} \rightarrow p\bar{p}) = (15.9 \pm 4.3 \pm 5.3) \times 10^{-5}$ , where the first error is statistical and the second one systematic. Branching fractions of  $\chi_{c0,2} \rightarrow \pi^+\pi^-$  and  $K^+K^-$  are also reported.

The hadronic decay rates of the  $P$ -wave quarkonium states provide tests of perturbative QCD. Recently, a systematic approach to the treatment of the infrared ambiguities in the calculation of the production and decays of these states has been developed [1]. However, existing experimental information on the triplet  $P$ -wave  $c\bar{c}$  states ( $\chi_{c0,1,2}$ ), especially the  $J = 0$   $\chi_{c0}$ , is not adequate for testing the predictions of this new theory.

In particular, the total width of the  $\chi_{c0}$  is a quantity of considerable interest. The two existing measurements have large errors and only marginal consistency [2]. Also of interest is the decay  $\chi_{c0} \rightarrow p\bar{p}$ , which is forbidden in the limit of massless helicity conservation [3] and has been calculated by many different models [4,5]. Here the only existing measurement is an upper limit on the partial width that does not seriously constrain the theory [6]. Calculations of the branching fractions for other exclusive  $\chi_{cJ}$  decays, such as  $\chi_{cJ} \rightarrow \pi^+\pi^-$  [7], has revealed orders-of-magnitude discrepancies with the data reported by early experiments. For these reasons, measurements of these properties of the  $\chi_{cJ}$  states with improved precision are very useful.

In this paper we report a measurement of  $\Gamma_{\chi_{c0}}^{tot}$  determined from an analysis of exclusive  $\psi(2S) \rightarrow \gamma\pi^+\pi^-$  and  $\gamma K^+K^-$  decays seen in the Beijing Spectrometer (BES) at the Beijing Electron Positron Collider (BEPC). We also report a first measurement of the  $\chi_{c0} \rightarrow p\bar{p}$  branching fraction, and improved precision on the branching fractions for  $\chi_{c0,2} \rightarrow \pi^+\pi^-$  and  $K^+K^-$ .

The BES is a conventional solenoidal magnet detector that is described in detail in Ref. [8]. A four-layer central drift chamber (CDC) surrounding the beampipe provides trigger information. A forty-layer main drift chamber (MDC), located radially outside the CDC, provides trajectory and energy loss ( $dE/dx$ ) information for charged tracks over 85% of the total solid angle. The momentum resolution is  $\sigma_p/p = 0.017\sqrt{1+p^2}$  ( $p$  in GeV/ $c$ ), and the  $dE/dx$  resolution for hadron tracks is  $\sim 11\%$ . An array of 48 scintillation counters surrounding the MDC measures the time of flight (TOF) of charged tracks with a resolution of  $\sim 450$  ps for hadrons. Radially outside the TOF system is a 12 radiation length, lead-gas barrel shower counter (BSC). This measures the energies of electrons and photons over  $\sim 80\%$  of the total solid angle with an energy resolution of  $\sigma_E/E = 22\%/\sqrt{E}$  ( $E$  in GeV). Outside of the solenoidal coil, which provides a 0.4 T magnetic field over the tracking volume, is an iron flux return that is instrumented with three double layers of counters that identify muons of momentum greater than 0.5 GeV/ $c$ .

We study  $\chi_c$  states produced by the reaction  $e^+e^- \rightarrow \psi(2S) \rightarrow \gamma\chi_c$  in a data sample corresponding to a total of  $3.79 \times 10^6$   $\psi(2S)$  decays [9]. For the  $\Gamma_{\chi_{c0}}^{tot}$  determination reported here we use the paired pseudoscalar meson decay modes of  $\chi_{c0,2} \rightarrow \pi^+\pi^-$  and  $K^+K^-$ . Using the particle identification capabilities of the detector and four-constraint kinematic fits, we can get relatively pure event samples. Moreover, since the decays of the  $\chi_{c1}$  and the  $\eta'_c$  to  $\pi^+\pi^-$  or  $K^+K^-$  are forbidden by parity conservation, the  $\chi_{c0}$  and  $\chi_{c2}$  signals in these channels are free of distortions due to possible contamination of these other states. The effects of cross-contamination between the  $\pi^+\pi^-$  and  $K^+K^-$  event samples are estimated by Monte Carlo (MC) simulations and corrected accordingly. The total width of the  $\chi_{c2}$  has been precisely measured to be  $\Gamma_{\chi_{c2}}^{tot} = 2.00 \pm 0.18$  MeV [10], which is much narrower than our experimental resolution at  $M_{\chi_{c2}}$  of 7.83 MeV. Thus, the strong  $\chi_{c2} \rightarrow \pi^+\pi^-$  signal in our data is used to provide a direct experimental determination of our resolution. We only rely on the MC simulation to determine how the resolution changes between  $M_{\chi_{c2}}$  and  $M_{\chi_{c0}}$ .

We select  $\psi(2S) \rightarrow \gamma\pi^+\pi^-$ ,  $\gamma K^+K^-$  and  $\gamma p\bar{p}$  by imposing the following selection criteria.

A cluster of deposited energy in the BSC is regarded as a photon candidate if: (1) the angle between the nearest charged track and the cluster in the  $r\phi$  plane is greater than  $15^\circ$ ; (2) the energy of the cluster is greater than 20 MeV and some energy is deposited in the first 6 radiation lengths of the counter; and (3) the angle determined from the cluster development in the BSC agrees with that determined from the relative position of the shower location and the interaction point to within  $37^\circ$ . At least one and at most three photon candidates are allowed in an event. The candidate with the largest BSC energy is assumed to be the photon radiated from the  $\psi(2S)$ .

In addition, we require that the event has two oppositely signed charged tracks in the MDC that both have at least 13 good hits and are well fit to a three-dimensional helix. Events with tracks where the  $dE/dx$  measured in the MDC and the shower properties in the BSC are consistent with electrons are rejected. For each track, the TOF and  $dE/dx$  measurements are used to assign probabilities that the particle is a pion, kaon and proton ( $Prob_\pi, Prob_K, Prob_p$ ). We require both tracks to have  $Prob_\pi > 0.01$  (for  $\pi^+\pi^-$ ) or  $Prob_K > 0.01$  (for  $K^+K^-$ ) or  $Prob_p > 0.05$  (for  $p\bar{p}$ ). In addition we do four-constraint kinematic fits to the hypotheses  $\psi(2S) \rightarrow \gamma\pi^+\pi^-$ ,  $\psi(2S) \rightarrow \gamma K^+K^-$  and  $\psi(2S) \rightarrow \gamma p\bar{p}$  and require the  $\chi^2$  probability of the fit  $P_{\chi^2}$  to be greater than 0.01 for  $\pi^+\pi^-$  or  $K^+K^-$  and greater than 0.05 for  $p\bar{p}$ .

There is some background from  $J/\psi \rightarrow \mu^+\mu^-$ , where the  $J/\psi$  is produced by cascade  $\psi(2S)$  to  $J/\psi$  decays. To reduce this, we reject events where the response of the muon detection system is consistent with the two charged tracks being muons. The surviving  $\mu^+\mu^-$  background events do not populate the  $\pi^+\pi^-$  invariant mass distribution near the  $\chi_{c0}$  or  $\chi_{c2}$  masses. In the  $K^+K^-$  mass distribution, however, they populate the region in the lower mass side of  $\chi_{c0}$ , and cause an abnormal distribution. For the  $p\bar{p}$  sample, the  $\mu^+\mu^-$  background level is significant. For this channel, in order to insure that both tracks are directed at the sensitive area of the muon detection system, we require  $|\cos\theta_{\text{MDC}}| < 0.65$  for both the  $p$  and the  $\bar{p}$  track.

To distinguish  $\gamma\pi^+\pi^-$  from  $\gamma K^+K^-$ , we define

$$Prob_{all}^{P^+P^-} = Prob(\chi_{all}^2, ndf_{all}),$$

where  $\chi_{all}^2 = \chi_{4C}^2 + \chi_{TOF}^2 + \chi_{dE/dx}^2$  and  $ndf_{all} = ndf_{4C} + ndf_{TOF} + ndf_{dE/dx}$  are the total  $\chi^2$  and the corresponding number of degrees of freedom of the  $\chi^2$  distribution. Here  $\chi_{4C}^2$ ,  $\chi_{TOF}^2$  and  $\chi_{dE/dx}^2$  correspond to the  $\chi^2$  values from the 4-constraint kinematic fit, the TOF measurements for the  $\pi$  or  $K$  hypothesis, and the  $dE/dx$  measurements for the  $\pi$  or  $K$  hypothesis, respectively, and  $ndf_{4C}$ ,  $ndf_{TOF}$  and  $ndf_{dE/dx}$  are the corresponding numbers of degrees of freedom. If  $Prob_{all}^{\pi^+\pi^-} > Prob_{all}^{K^+K^-}$ , the event is categorized as a  $\gamma\pi^+\pi^-$  event, and if  $Prob_{all}^{K^+K^-} > Prob_{all}^{\pi^+\pi^-}$ , it is categorized as a  $\gamma K^+K^-$  event.

Figures 1 and 2 show the  $\pi^+\pi^-$  and  $K^+K^-$  invariant mass distributions after the imposition of all the above-listed selection requirements. In these plots, the mass values corresponding to the  $\chi_{c0}$  and  $\chi_{c2}$  peaks are lower in the  $\pi^+\pi^-$  channel and higher for  $K^+K^-$ , indicating the presence of some remaining cross contamination between the two samples, which must be accounted for in the determination of the  $\chi_{c0}$  parameters. From Fig. 2, it is apparent that the  $\chi_{c2} \rightarrow K^+K^-$  sample is statistically limited. We therefore use only

the  $\chi_{c2} \rightarrow \pi^+\pi^-$  signal to calibrate the mass resolution. In Fig. 3, the  $p\bar{p}$  invariant mass distribution, there is a clear  $\chi_{c0}$  signal and evidence for the  $\chi_{c1}$  and  $\chi_{c2}$ .

We use Monte Carlo simulated data to determine the  $\pi^+\pi^-$  and  $K^+K^-$  cross contamination probabilities, the detection efficiencies and the mass resolutions. We generate events assuming that the reaction  $\psi(2S) \rightarrow \gamma\chi_{cJ}$  is a pure E1 transition. The decays  $\chi_{cJ} \rightarrow$  pseudoscalar meson pairs and  $\chi_{c0} \rightarrow p\bar{p}$  have only one independent helicity amplitude and are thus unambiguous [11]. For  $\chi_{c1,2} \rightarrow p\bar{p}$  decays, there are no available experimental data on the helicity amplitudes, and we use an isotropic distribution. (Our  $p\bar{p}$  event samples are too small to permit a helicity amplitude analysis.)

We subject the MC-generated events to the same selection process as is used for the data and determine the detection efficiencies for each mode. For the  $p\bar{p}$  mode, the detection efficiencies and the error caused by the limited statistics of the Monte Carlo sample are  $\varepsilon_{\chi_{c0}} = (27.1 \pm 0.6)\%$ ,  $\varepsilon_{\chi_{c1}} = (30.3 \pm 0.7)\%$  and  $\varepsilon_{\chi_{c2}} = (27.6 \pm 0.6)\%$ , and mass resolutions at the  $\chi_{c0}$ ,  $\chi_{c1}$  and  $\chi_{c2}$  equal to 7.3, 6.8 and 6.7 MeV, respectively. For the  $\pi^+\pi^-$  and  $K^+K^-$  modes, the simulation shows that the mass dependence of the detection efficiency is small and the mass resolution function is very nearly Gaussian. We compensate for the distortion of the mass spectra due to the  $\pi^+\pi^-K^+K^-$  cross contamination by calibrating the mass resolution derived from the MC simulation with the  $\chi_{c2} \rightarrow \pi^+\pi^-$  line shape seen with the data. The efficiencies are  $\varepsilon_{\chi_{c0} \rightarrow \pi^+\pi^-} = (36.9 \pm 0.3)\%$ ,  $\varepsilon_{\chi_{c2} \rightarrow \pi^+\pi^-} = (38.9 \pm 0.5)\%$ ,  $\varepsilon_{\chi_{c0} \rightarrow K^+K^-} = (32.8 \pm 0.3)\%$  and  $\varepsilon_{\chi_{c2} \rightarrow K^+K^-} = (34.9 \pm 0.5)\%$ , and the probability for  $\chi_{c0}$  ( $\chi_{c2}$ )  $\rightarrow K^+K^-$  events to be categorized as  $\pi^+\pi^-$  is  $(5.6 \pm 0.2)\%$  ( $(6.0 \pm 0.2)\%$ ), and that for  $\chi_{c0}$  ( $\chi_{c2}$ )  $\rightarrow \pi^+\pi^-$  events to be selected as  $K^+K^-$  is  $(7.1 \pm 0.2)\%$  ( $(7.4 \pm 0.3)\%$ ), where the error is from the statistics of the Monte Carlo sample.

The invariant mass distributions in Figs. 1, 2 and 3 are fit by using an unbinned maximum likelihood algorithm. For the  $p\bar{p}$  channel, the invariant mass region between 3.20 and 3.64 GeV is fit with three Breit-Wigner resonances plus a linear background function. The Breit-Wigner resonance width for the  $\chi_{c0}$  is fixed at 14.3 MeV, the value determined from an analysis of  $\chi_{c0} \rightarrow \pi^+\pi^-$  decays described below; those for the  $\chi_{c1}$  and  $\chi_{c2}$  are fixed at the PDG values [10]. The resonances are smeared by Gaussian functions with rms widths fixed at the MC-determined mass resolution values. The fit result, shown as the curve in Fig. 3, gives  $15.2 \pm 4.1$ ,  $4.2 \pm 2.2$  and  $4.7 \pm 2.5$  events for the  $\chi_{c0}$ ,  $\chi_{c1}$  and  $\chi_{c2}$  states, respectively.

For the  $\pi^+\pi^-$  channel, we first fit the invariant mass region between 3.5 and 3.6 GeV with a Breit-Wigner resonance with  $\Gamma_{\chi_{c2}}$  fixed at the PDG value of 2.00 MeV, smeared by a Gaussian resolution function with an rms width that is allowed to float. We also include a linear background function. The fit results in a  $\chi_{c2}$  mass resolution of  $7.83 \pm 1.04$  MeV, which is slightly higher than the MC result of  $6.31 \pm 0.11$  MeV. We scale the MC value for the mass resolution at the  $\chi_{c0}$  ( $8.12 \pm 0.23$  MeV) by the ratio of the fitted MC results at the  $\chi_{c2}$  and get a mass resolution at the  $\chi_{c0}$  of 10.08 MeV.

We then fit the  $\pi^+\pi^-$  mass spectrum between 3.2 and 3.6 GeV with two Gaussian-smeared Breit-Wigners with resolutions fixed at 10.08 and 7.83 MeV, and a second order polynomial background function, and with  $\Gamma_{\chi_{c2}}$  fixed at the PDG value of 2.00 MeV. The fit, shown as the curve in Fig. 1, gives  $\Gamma_{\chi_{c0}} = 14.3 \pm 2.0$  MeV, where the error is statistical. The fitted numbers of  $\chi_{cJ} \rightarrow \pi^+\pi^-$  events are  $n_{\chi_{c0} \rightarrow \pi^+\pi^-}^{obs} = 720 \pm 32$  and  $n_{\chi_{c2} \rightarrow \pi^+\pi^-}^{obs} = 185 \pm 16$ , where the errors are statistical.

We fit the  $K^+K^-$  mass spectrum between 3.2 and 3.6 GeV to two Gaussian-smeared

Breit-Wigner resonance functions plus a background function that includes the possibility of distortions to the line shape due to  $\mu^+\mu^-X$  background events. (Because this mode is not used for width determination, a high precision knowledge of the mass resolution is not an issue.) The  $\chi_{c2}$  width is fixed. The resulting fit, shown in Fig. 2, gives  $n_{\chi_{c0}\rightarrow K^+K^-}^{obs} = 774 \pm 38$  and  $n_{\chi_{c2}\rightarrow K^+K^-}^{obs} = 115 \pm 13$ , where the errors are statistical.

Errors in the determination of  $\Gamma_{\chi_{c0}}$  are caused by the uncertainty in  $\Gamma_{\chi_{c2}}$ , the determination of the mass resolution, the shape of the background, the mass dependence of the efficiency correction, and the choice of experimental cuts. We add the estimated errors from these sources in quadrature and get a total relative systematic error on  $\Gamma_{\chi_{c0}}$  of 21%.

Systematic errors on the branching fractions, which arise from the uncertainties in  $\Gamma_{\chi_{c2}}$ , the mass resolution, the choice of the background function, the efficiency determination, and the choices of the selection criteria are 11.5%, 12.6%, 12.1% and 14.7% for  $B(\chi_{c0} \rightarrow \pi^+\pi^-)$ ,  $B(\chi_{c0} \rightarrow K^+K^-)$ ,  $B(\chi_{c2} \rightarrow \pi^+\pi^-)$  and  $B(\chi_{c2} \rightarrow K^+K^-)$ , respectively. There are overall errors caused by the uncertainty of the total number of  $\psi(2S)$  events and the uncertainties in the  $\psi(2S) \rightarrow \gamma\chi_{cJ}$  branching fractions. Adding these errors in quadrature gives total relative systematic errors of 14%, 15%, 15% and 16%, respectively, for  $B(\chi_{c0} \rightarrow \pi^+\pi^-)$ ,  $B(\chi_{c0} \rightarrow K^+K^-)$ ,  $B(\chi_{c2} \rightarrow \pi^+\pi^-)$  and  $B(\chi_{c2} \rightarrow K^+K^-)$ .

For  $B(\chi_{cJ} \rightarrow p\bar{p})$ , sources of systematic errors include those listed above plus that associated with the assumption of an isotropic angular distribution for  $\chi_{c1,2} \rightarrow p\bar{p}$  decays. Adding all of the errors in quadrature gives relative systematic errors of 33%, 67% and 56% for the  $\chi_{c0}$ ,  $\chi_{c1}$  and  $\chi_{c2}$  states, respectively.

In summary, we obtain the total width of the  $\chi_{c0}$  to be

$$\Gamma_{\chi_{c0}} = 14.3 \pm 2.0 \pm 3.0 \text{ MeV},$$

where the first error is statistical and the second is systematic. The  $\chi_{cJ}$  branching fraction results are listed in Table I and Table II. The measured width for the  $\chi_{c0}$  is consistent with but substantially more precise than the previous measurement [2] (the uncertainty is reduced from 40% to 25%). The calculations involving new factorization schemes with high order QCD corrections [12,13] are in good agreement with our measurement.

Our branching fraction for  $\chi_{c0} \rightarrow p\bar{p}$  is the first measurement for this decay, and is compatible with the previous upper bound [6]. Our results for  $\chi_{c1,2} \rightarrow p\bar{p}$  decays, although statistically limited, are consistent, within errors, with the values determined from studies of charmonium states formed directly in  $p\bar{p}$  annihilation [14]. The calculation with mass correction effect [4] gives much smaller value of  $\Gamma(\chi_{c0} \rightarrow p\bar{p})$  than our result while the model considering the diquark content of the proton [5] can find result consistent with our measurement.

Finally, our branching fractions for  $\chi_{c0,2}$  decays into  $\pi^+\pi^-$  and  $K^+K^-$  are somewhat lower than the existing world average [10]. Recent calculations of exclusive  $\chi_{cJ}$  decays that include contributions from color-octet processes [15] are in generally good agreement with our measurements. Using our results and canceling out the common errors in the branching fractions, we get the ratios of the branching fractions of  $\frac{B(\chi_{c0}\rightarrow\pi^+\pi^-)}{B(\chi_{c0}\rightarrow K^+K^-)} = 0.82 \pm 0.15$  and

$$\frac{B(\chi_{c2}\rightarrow\pi^+\pi^-)}{B(\chi_{c2}\rightarrow K^+K^-)} = 1.88 \pm 0.51.$$

We thank the staffs of the BEPC Accelerator and the Computing Center at the Institute of High Energy Physics, Beijing, for their outstanding scientific efforts. This project was

partly supported by China Postdoctoral Science Foundation. The work of the BES Collaboration was supported in part by the National Natural Science Foundation of China under Contract No. 19290400 and the Chinese Academy of Sciences under contract No. KJ85 (IHEP), and by the Department of Energy under Contract Nos. DE-FG03-92ER40701 (Caltech), DE-FG03-93ER40788 (Colorado State University), DE-AC03-76SF00515 (SLAC), DE-FG03-91ER40679 (UC Irvine), DE-FG03-94ER40833 (U Hawaii), DE-FG03-95ER40925 (UT Dallas).

## REFERENCES

<sup>†</sup> Deceased.

- [1] G. T. Bodwin, E. Braaten and G. P. Lepage, Phys. Rev. **D51**, 1125 (1995).
- [2] J. E. Gaiser *et al.*, Phys. Rev. **D34**, 711 (1986).
- [3] S. J. Brodsky and G. P. Lepage, Phys. Rev. **D24**, 2848 (1981).
- [4] M. Anselmino, R. Cancelliere and F. Murgia, Phys. Rev. **D46**, 5049 (1992).
- [5] M. Anselmino, F. Caruso and S. Forte, Phys. Rev. **D44**, 1438 (1991); M. Anselmino and F. Murgia, Z. Phys. **C58**, 429 (1993).
- [6] R. Brandelik *et al.*, Nucl. Phys. **B160**, 426 (1979).
- [7] V. L. Chernyak and A. R. Zhitnitsky, Phys. Rep. **112**, 173 (1984).
- [8] J. Z. Bai *et al.*, (BES Collab.), Nucl. Instr. Meth. **A344**, 319 (1994).
- [9] J. Z. Bai *et al.*, (BES Collab.), hep-ex/9806012, Phys. Rev. **D** (to be published).
- [10] R. M. Barnett *et al.*, (Particle Data Group), Phys. Rev. **D54** part I (1996) and references therein.
- [11] P. K. Kabir and A. J. G. Hey, Phys. Rev. **D13**, 3161 (1976).
- [12] Han-Wen Huang and Kuang-Ta Chao, Phys. Rev. **D54**, 6850 (1996).
- [13] M. L. Mangano and A. Petrelli, Phys. Lett. **B352**, 445 (1995); A. Petrelli, Phys. Lett. **B380**, 159 (1996).
- [14] T. A. Armstrong *et al.*, Nucl. Phys. **B373**, 35 (1992); C. Baglin *et al.*, Phys. Lett. **B172**, 455 (1986);
- [15] J. Bolz, P. Kroll and G. A. Schuler, Phys. Lett. **B392**, 198 (1997).

## FIGURES

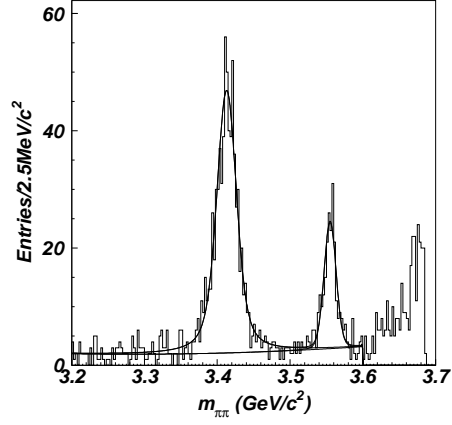


FIG. 1. The  $\pi^+\pi^-$  mass distribution for selected  $\psi(2S) \rightarrow \gamma\pi^+\pi^-$  events.

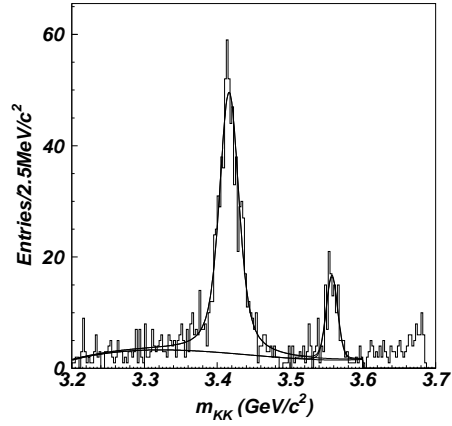


FIG. 2. The  $K^+K^-$  mass distribution for selected  $\psi(2S) \rightarrow \gamma K^+K^-$  events.

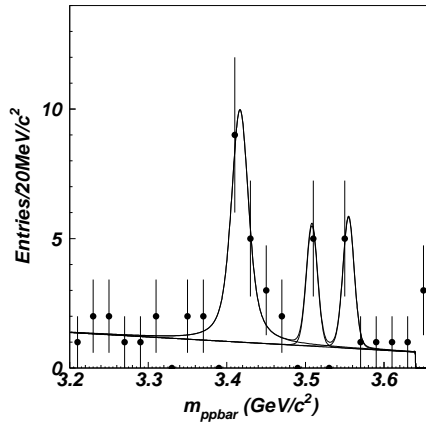


FIG. 3. The  $p\bar{p}$  mass distribution for selected  $\psi(2S) \rightarrow \gamma p\bar{p}$  events.

TABLES

TABLE I. Branching fractions of  $\chi_{cJ} \rightarrow 0^-0^-$ .  $B(\psi(2S) \rightarrow \gamma\chi_{c0}) = (9.3 \pm 0.8)\%$  and  $B(\psi(2S) \rightarrow \gamma\chi_{c2}) = (7.8 \pm 0.8)\%$  are used for branching fractions determination.

decay mode	$N^{obs}$	BR( $\times 10^{-3}$ )	PDG [10] ( $10^{-3}$ )
$\chi_{c0} \rightarrow \pi^+\pi^-$	$720 \pm 32$	$4.68 \pm 0.26 \pm 0.65$	$7.5 \pm 2.1$
$\chi_{c0} \rightarrow K^+K^-$	$774 \pm 38$	$5.68 \pm 0.35 \pm 0.85$	$7.1 \pm 2.4$
$\chi_{c2} \rightarrow \pi^+\pi^-$	$185 \pm 16$	$1.49 \pm 0.14 \pm 0.22$	$1.9 \pm 1.0$
$\chi_{c2} \rightarrow K^+K^-$	$115 \pm 13$	$0.79 \pm 0.14 \pm 0.13$	$1.5 \pm 1.1$

TABLE II. Branching ratios of  $\chi_{cJ} \rightarrow p\bar{p}$ .  $B(\psi(2S) \rightarrow \gamma\chi_{c0}) = (9.3 \pm 0.8)\%$ ,  $B(\psi(2S) \rightarrow \gamma\chi_{c1}) = (8.7 \pm 0.8)\%$  and  $B(\psi(2S) \rightarrow \gamma\chi_{c2}) = (7.8 \pm 0.8)\%$  are used for branching fractions determination.  $\Gamma_{\chi_{c0}}^{tot}$  from this experiment,  $\Gamma_{\chi_{c1}}^{tot} = 0.88 \pm 0.14$  MeV and  $\Gamma_{\chi_{c2}}^{tot} = 2.00 \pm 0.18$  MeV are used in calculating the partial widths.

state	$N^{obs}$	BR( $\times 10^{-5}$ )	$\Gamma_{p\bar{p}}$ (keV)	PDG [10] BR( $10^{-5}$ )	PDG [10] $\Gamma_{p\bar{p}}$ (keV)
$\chi_{c0}$	$15.2 \pm 4.1$	$15.9 \pm 4.3 \pm 5.3$	$2.3 \pm 1.1$	$< 90$	—
$\chi_{c1}$	$4.2 \pm 2.2$	$4.2 \pm 2.2 \pm 2.8$	$0.037 \pm 0.032$	$8.6 \pm 1.2$	$0.074 \pm 0.009$
$\chi_{c2}$	$4.7 \pm 2.5$	$5.8 \pm 3.1 \pm 3.2$	$0.116 \pm 0.090$	$10.0 \pm 1.0$	$0.206 \pm 0.022$